

## Doping and temperature dependence of incommensurate antiferromagnetism in underdoped lanthanum cuprates

Feng Yuan and Shiping Feng

Department of Physics, Beijing Normal University, Beijing 100875, China;  
 Institute of Theoretical Physics, Academia Sinica, Beijing 100080, China;  
 and National Laboratory of Superconductivity, Academia Sinica, Beijing 100080, China

Zhao-Bin Su

Institute of Theoretical Physics, Academia Sinica, Beijing 100080, China

Lu Yu

The Abdus Salam International Centre for Theoretical Physics, 34014 Trieste, Italy  
 and Institute of Theoretical Physics, Academia Sinica, Beijing 100080, China

(Received 10 May 2001; published 20 November 2001)

The doping, temperature, and energy dependence of the dynamical spin structure factors of the underdoped lanthanum cuprates in the normal state are studied within the  $t$ - $J$  model using the fermion-spin transformation technique. Incommensurate peaks are found at  $[(1 \pm \delta)\pi, \pi]$ ,  $[\pi, (1 \pm \delta)\pi]$  at relatively low temperatures, with  $\delta$  linearly increasing with doping at the beginning and then saturating at higher dopings. These peaks broaden and weaken in amplitude with temperature and energy, in good agreement with experiments. The theory also predicts a rotation of these peaks by  $\pi/4$  at even higher temperatures, being shifted to  $[(1 \pm \delta/\sqrt{2})\pi, (1 \pm \delta/\sqrt{2})\pi]$ .

DOI: 10.1103/PhysRevB.64.224505

PACS number(s): 74.72.Dn, 74.25.Ha, 74.20.Mn

In spite of the tremendous efforts dedicated to the studies of anomalous properties of high- $T_c$  superconductors, many important problems still remain open. Among others, the destruction of antiferromagnetic long range order (AFLRO) and appearance of incommensurate antiferromagnetism (IAF) in doped cuprates is one of the challenging issues for the theory of strongly correlated electron systems. Moreover, the interplay of AF and superconductivity in these compounds is of fundamental importance for the high- $T_c$  theory. Experimentally, by virtue of systematic studies using NMR and  $\mu$ SR techniques, particularly the inelastic neutron scattering, rather detailed information on dynamical magnetic properties has become available now, awaiting an adequate theoretical interpretation. It has been established that beyond certain critical doping ( $\sim 3\%$ ) the commensurate AFLRO disappears, being replaced by IAF, characterized by incommensurability parameters  $\delta$ , i.e., the AF Bragg peaks are shifted from  $[\pi, \pi]$  to four points  $[\pi(1 \pm \delta), \pi]$ ,  $[\pi, (1 \pm \delta)\pi]$ .<sup>1</sup> For very low dopings  $\delta$  varies almost linearly with concentration  $x$ , but saturates at higher dopings. These peaks broaden and weaken in amplitude as the temperature and energy increase. These features are fully confirmed by the data on lanthanum cuprates,<sup>1-4</sup> and have also been found recently on yttrium cuprates.<sup>5</sup> Theoretically there is a general consensus that IAF emerges due to doped charge carriers. Several attempts have been made to make this argument more precise, including the hole induced frustration,<sup>6</sup> stripe formation,<sup>7</sup> spiral phase,<sup>8</sup> and Fermi surface nesting.<sup>9</sup> Based on the phenomenological ansatz of marginal Fermi liquid behavior<sup>10</sup> and tight binding calculation, a detailed fitting of the experimental data was attempted.<sup>11</sup> Recently experiments show stronger singularities of AF fluctuations<sup>12</sup> than what is anticipated from the phenomenological models. The proxim-

ity to a quantum critical point<sup>13</sup> was proposed as an alternative explanation.<sup>12</sup> However, to the best of our knowledge, no systematic calculations have been performed within the standard strong correlation models for the dynamical spin structure factors (DSSF) to confront the experimental data. Exact diagonalization is limited by system sizes, while the quantum Monte Carlo technique faces the negative sign problem for lower temperatures.<sup>14</sup> Thus it is rather difficult to obtain conclusive results.

In this paper, using the fermion-spin theory<sup>15</sup> which implements properly the local single occupancy constraint, we calculate explicitly DSSF for cuprates within the  $t$ - $J$  model and reproduce all main features found in experiments,<sup>2-4,12</sup> including peak position as well as temperature and energy dependence. Apart from the ratio  $t/J$  (taken to be 2.5), there are no other adjustable parameters in the calculations. Moreover, the theory predicts the magnetic peaks will be rotated by  $\pi/4$  at even higher temperatures, i.e., being shifted to  $[(1 \pm \delta/\sqrt{2})\pi, (1 \pm \delta/\sqrt{2})\pi]$ . To avoid complications due to bilayers we will focus on the normal state IAF in lanthanum cuprates.

We start from the  $t$ - $J$  model on a square lattice

$$H = -t \sum_{i\hat{\eta}\sigma} C_{i\sigma}^\dagger C_{i+\hat{\eta}\sigma} + \text{H.c.} - \mu \sum_{i\sigma} C_{i\sigma}^\dagger C_{i\sigma} + J \sum_{i\hat{\eta}} \mathbf{S}_i \cdot \mathbf{S}_{i+\hat{\eta}}, \quad (1)$$

with the local constraint  $\sum_{\sigma} C_{i\sigma}^\dagger C_{i\sigma} \leq 1$ , where  $\hat{\eta} = \pm \hat{x}, \pm \hat{y}$ , and  $\mathbf{S}_i = C_i^\dagger \vec{\sigma} C_i / 2$  are spin operators with  $\vec{\sigma} = (\sigma_x, \sigma_y, \sigma_z)$  as Pauli matrices. The single occupancy local constraint can be treated *properly in analytical form* within the fermion-spin theory<sup>15</sup> based on the slave particle approach,<sup>16</sup>  $C_{i\uparrow}$

$=h_i^\dagger S_i^-, C_{i\downarrow}=h_i^\dagger S_i^+$ , where the spinless fermion operator  $h_i$  describes the charge (holon) degrees of freedom, while the pseudospin operator  $S_i$  describes the spin (spinon) degrees of freedom. In this representation, the *low-energy* Hamiltonian of the  $t$ - $J$  model (1) can be rewritten as<sup>15</sup>

$$H = t \sum_{i\hat{\eta}} h_{i+\hat{\eta}}^\dagger h_i (S_i^+ S_{i+\hat{\eta}}^- + S_i^- S_{i+\hat{\eta}}^+) + \mu \sum_i h_i^\dagger h_i + J_{\text{eff}} \sum_{i\hat{\eta}} (\mathbf{S}_i \cdot \mathbf{S}_{i+\hat{\eta}}), \quad (2)$$

with  $J_{\text{eff}} = J[(1-x)^2 - \phi^2]$ , where  $x$  is the hole doping concentration, the holon hopping parameter  $\phi = \langle h_i^\dagger h_{i+\hat{\eta}} \rangle$ , and  $S_i^+$  and  $S_i^-$  as the pseudospin raising and lowering operators, respectively. It has been shown<sup>15</sup> that the constrained electron operator can be mapped exactly using the fermion-spin transformation defined with an additional projection operator. However, this projection operator is cumbersome to handle in the actual calculations, and we have not presented it explicitly in Eq. (2). It has also been shown<sup>15</sup> that such treatment leads to errors of the order  $x$  in counting the number of spin states, which is negligible for small dopings. Within this framework the spin fluctuations only couple to spinons, but the strong correlation between holons and spinons is included self-consistently through the holon's parameters entering the spinon propagator. Therefore both spinons and holons are responsible for the spin dynamics. The universal behavior of the momentum-integrated DSSF and susceptibility in the underdoped regime has been calculated within the fermion-spin theory<sup>17</sup> by considering spinon fluctuations around the mean-field (MF) solution, where the spinon part is treated by the loop expansion to the second order. Following Ref. 17, we obtain DSSF as

$$S(\mathbf{k}, \omega) = -2[1 + n_B(\omega)] \text{Im} D(\mathbf{k}, \omega) = -2[1 + n_B(\omega)] \times \frac{B_k^2 \text{Im} \Sigma_s^{(2)}(\mathbf{k}, \omega)}{[\omega^2 - \omega_k^2 - B_k \text{Re} \Sigma_s^{(2)}(\mathbf{k}, \omega)]^2 + [B_k \text{Im} \Sigma_s^{(2)}(\mathbf{k}, \omega)]^2}, \quad (3)$$

where the full spinon Green's function  $D^{-1}(\mathbf{k}, \omega) = D^{(0)-1}(\mathbf{k}, \omega) - \Sigma_s^{(2)}(\mathbf{k}, \omega)$ , with the MF spinon Green's function<sup>18</sup>  $D^{(0)-1}(\mathbf{k}, \omega) = (\omega^2 - \omega_k^2)/B_k$ , while  $\text{Im} \Sigma_s^{(2)}(\mathbf{k}, \omega)$  and  $\text{Re} \Sigma_s^{(2)}(\mathbf{k}, \omega)$  are the imaginary and real parts of the second order spinon self-energy, respectively, obtained from the holon bubble

$$\Sigma_s^{(2)}(\mathbf{k}, \omega) = - \left( \frac{Zt}{N} \right)^2 \sum_{pp'} (\gamma_{p'+p+k} + \gamma_{k-p'})^2 \times \frac{B_{k+p}}{2\omega_{k+p}} \left( \frac{F_1(k, p, p')}{\omega + \xi_{p+p'} - \xi_{p'} + \omega_{k+p}} - \frac{F_2(k, p, p')}{\omega + \xi_{p+p'} - \xi_{p'} - \omega_{k+p}} \right), \quad (4)$$

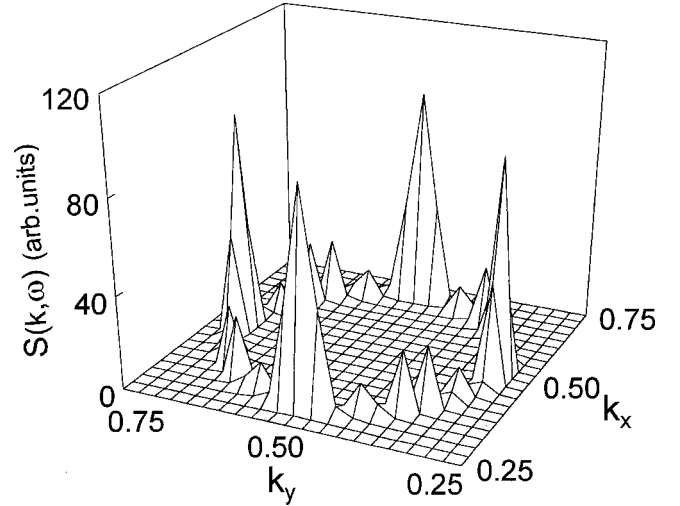


FIG. 1. The dynamical spin structure factor in the  $(k_x, k_y)$  plane at doping  $x=0.06$ , temperature  $T=0.1J$ , and energy  $\omega=0.05J$  for parameter  $t/J=2.5$ .

where  $\gamma_{\mathbf{k}} = (1/Z) \sum_{\hat{\eta}} e^{i\mathbf{k} \cdot \hat{\eta}}$ ,  $Z$  is the coordination number,  $B_k = \Delta [2\chi_z(\epsilon\gamma_k - 1) + \chi(\gamma_k - \epsilon)]$ ,  $\Delta = 2ZJ_{\text{eff}}$ ,  $\epsilon = 1 + 2t\phi/J_{\text{eff}}$ ,  $F_1(k, p, p') = n_F(\xi_{p+p'})[1 - n_F(\xi_{p'})] + [1 + n_B(\omega_{k+p})][n_F(\xi_{p'}) - n_F(\xi_{p+p'})]$ ,  $F_2(k, p, p') = n_F(\xi_{p+p'})[1 - n_F(\xi_{p'})] - n_B(\omega_{k+p})[n_F(\xi_{p'}) - n_F(\xi_{p+p'})]$ ,  $n_F(\xi_k)$ , and  $n_B(\omega_k)$  are the fermion and boson distribution functions, respectively, the MF holon excitation  $\xi_k = 2Zt\chi\gamma_k + \mu$ , and the MF spinon excitation  $\omega_k^2 = \Delta^2(A_1\gamma_k^2 + A_2\gamma_k + A_3)$  with  $A_1 = \alpha\epsilon(\chi/2 + \epsilon\chi_z)$ ,  $A_2 = \epsilon[(1-Z)\alpha(\epsilon\chi/2 + \chi_z)/Z - \alpha(C_z + C/2) - (1-\alpha)/(2Z)]$ ,  $A_3 = \alpha(C_z + \epsilon^2 C/2) + (1-\alpha)(1+\epsilon^2)/(4Z) - \alpha\epsilon(\chi/2 + \epsilon\chi_z)/Z$ , the spinon correlation functions  $\chi = \langle S_i^+ S_{i+\hat{\eta}}^- \rangle$ ,  $\chi_z = \langle S_i^z S_{i+\hat{\eta}}^z \rangle$ ,  $C = (1/Z^2) \sum_{\hat{\eta}\hat{\eta}'} \langle S_{i+\hat{\eta}}^+ S_{i+\hat{\eta}'}^- \rangle$ , and  $C_z = (1/Z^2) \sum_{\hat{\eta}\hat{\eta}'} \langle S_{i+\hat{\eta}}^z S_{i+\hat{\eta}'}^z \rangle$ . In order to satisfy the sum rule for the correlation function  $\langle S_i^+ S_i^- \rangle = 1/2$  in the absence of AFLRO, a decoupling parameter  $\alpha$  has been introduced in the MF calculation, which can be regarded as the vertex correction.<sup>18,19</sup> These MF order parameters  $\chi$ ,  $C$ ,  $\chi_z$ ,  $C_z$ ,  $\phi$ , and decoupling parameter  $\alpha$  have been determined<sup>18</sup> by the self-consistent equations.

Of course, at vanishing dopings the AFLRO gives rise to a commensurate peak at  $[1/2, 1/2]$  (hereafter we use the units of  $[2\pi, 2\pi]$ ), which is not presented here for the sake of space. Instead, we plot DSSF  $S(\mathbf{k}, \omega)$  in the  $(k_x, k_y)$  plane at doping  $x=0.06$ , temperature  $T=0.1J$  and energy  $\omega=0.05J$  for  $t/J=2.5$  in Fig. 1. The commensurate peak is split into four IAF peaks at  $[(1 \pm \delta)/2, 1/2]$  and  $[1/2, (1 \pm \delta)/2]$ . The calculated DSSF  $S(\mathbf{k}, \omega)$  has been used to extract the doping dependence of the incommensurability parameter  $\delta(x)$ , defined as the deviation of the peak position from the AF wave vector  $[1/2, 1/2]$ , and the result is shown in Fig. 2 in comparison with the experimental data<sup>4</sup> taken on  $\text{La}_{2-x}\text{Sr}_x\text{CuO}_4$  (inset).  $\delta(x)$  increases almost linearly with the hole concentration in the low-doping regime, but it saturates at higher dopings, in full agreement with experimental data.

For a better understanding of the IAF we have made a series of scans for  $S(\mathbf{k}, \omega)$  at different temperatures and energies, and the result for doping  $x=0.06$ ,  $t/J=2.5$  at  $T$

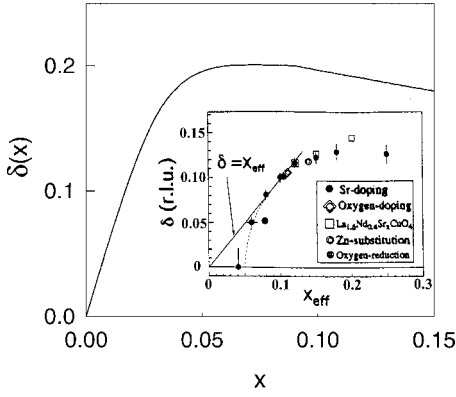


FIG. 2. The doping dependence of the incommensurability  $\delta(x)$  of the antiferromagnetic fluctuations. Inset: the experimental result on  $\text{La}_{2-x}\text{Sr}_x\text{CuO}_4$  taken from Ref. 4.

$=0.1J$  and  $\omega=0.1J$  is shown in Fig. 3. Comparing it with Fig. 1 for the same set of parameters except for  $\omega=0.05J$ , we see that at relatively low temperatures ( $T=0.1J$ ), although the positions of IAF peaks are almost energy independent, these peaks are broadened and suppressed with increasing energy, and tend to vanish at high energies. This reflects that the spin excitations are rather sharp in momentum space at low temperatures and energies, then the linewidth, or the inverse lifetime increases with increasing energy, in full agreement with experiments.<sup>4,12</sup> Now we turn to discuss the temperature dependence of  $S(\mathbf{k}, \omega)$ .  $S(\mathbf{k}, \omega)$  at  $x=0.06$  for  $t/J=2.5$  and  $\omega=0.05J$  at temperature  $T=0.5J$  is plotted in Fig. 4. To our big surprise, comparing it with Fig. 1 for the same set of parameters except for  $T=0.1J$ , we find that, apart from the suppression of the peak weight with temperature as anticipated, the positions of IAF peaks are temperature dependent, i.e., these peaks deviate from  $[(1 \pm \delta)/2, 1/2]$  and  $[1/2, (1 \pm \delta)/2]$  with increasing temperature, and are rotated by  $\pi/4$  in the reciprocal space about  $(1/2, 1/2)$  at higher temperatures ( $T \geq 0.5J$ ), being shifted to  $[(1 \pm \delta/\sqrt{2})/2, (1 \pm \delta/\sqrt{2})/2]$ . Up to now most experimental data show that the positions of IAF peaks in  $\text{La}_{2-x}\text{Sr}_x\text{CuO}_4$  (Refs. 4,12) and  $\text{La}_2\text{SrCuO}_{4+x}$  (Ref. 20) are located at  $[(1 \pm \delta)/2, 1/2]$  and  $[1/2, (1 \pm \delta)/2]$  in the underdoped regime, but these data in the normal-state are obtained at relatively

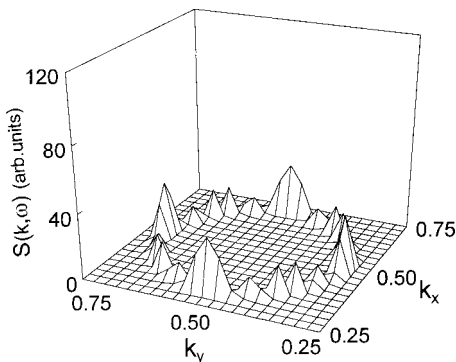


FIG. 3. The dynamical spin structure factor in the  $(k_x, k_y)$  plane at doping  $x=0.06$  for parameter  $t/J=2.5$  and energy  $\omega=0.1J$  at temperature  $T=0.1J$ .

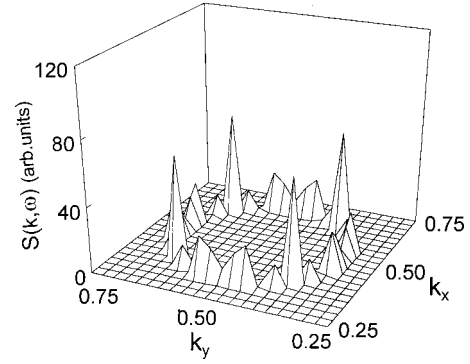


FIG. 4. The dynamical spin structure factor in the  $(k_x, k_y)$  plane at doping  $x=0.06$  for parameter  $t/J=2.5$  and energy  $\omega=0.05J$  at temperature  $T=0.5J$ .

low temperatures (near the superconducting transition). However, a strong temperature dependence  $S(\mathbf{k}, \omega)$  in  $\text{La}_{2-x}\text{Sr}_x\text{CuO}_4$  has been observed,<sup>4,12</sup> namely, the weight of IAF peaks at  $[(1 \pm \delta)/2, 1/2]$  and  $[1/2, (1 \pm \delta)/2]$  is suppressed severely with increasing temperature, whereas the weight is increasing with temperature<sup>12</sup> at  $[(1 \pm \delta/2)/2, (1 \pm \delta/2)/2]$ . This tendency is consistent with our theoretical predictions. Experiments at even higher temperatures are required to check our predictions explicitly.

Now we give some physical interpretation to the above obtained results. As seen from Eq. (3), the DSSF has a well-defined resonance character.  $S(\mathbf{k}, \omega)$  exhibits a peak when the incoming neutron energy  $\omega$  is equal to the renormalized spin excitation  $E_k^2 = \omega_k^2 + B_k \text{Re} \Sigma_s^{(2)}(k, E_k)$ , i.e.,  $W(\mathbf{k}_\delta, \omega) \equiv [\omega^2 - \omega_{k_\delta}^2 - B_{k_\delta} \text{Re} \Sigma_s^{(2)}(\mathbf{k}_\delta, \omega)]^2 = (\omega^2 - E_{k_\delta}^2)^2 \sim 0$  for certain critical wave vectors  $\mathbf{k}_\delta$  (positions of IAF peaks). The height of these peaks is determined by the imaginary part of the spinon self-energy, i.e.,  $1/\text{Im} \Sigma_s^{(2)}(\mathbf{k}_\delta, \omega)$ . Near half-filling, the spin excitations are centered around the AF wave vector  $[1/2, 1/2]$ , so the commensurate AF peak appears there. Upon doping, the holes disturb the AF background. Within the fermion-spin framework, as a result of self-consistent motion of holons and spinons, IAF is developed beyond certain critical doping, which means, the low-energy spin excitations drift away from the AF wave vector, or the zero of  $W(\mathbf{k}_\delta, \omega)$  is shifted from  $[\pi, \pi]$  to  $\mathbf{k}_\delta$ . As seen from Eq. (3), the physics is dominated by the spinon self-energy renormalization due to holons. In this sense, the mobile holes are the key factor leading to IAF. As seen from Fig. 5, function  $W(\mathbf{k}, \omega)$  has a rather deep valley along a circle of radius  $\delta$  around  $[1/2, 1/2]$ . However, if we enlarge the scale very significantly (by a factor of 300), as shown in Fig. 6, there is a strong angular dependence with actual minima (not exactly zero due to precision limitations) at  $[(1 - \delta)/2, 1/2]$  and  $[1/2, (1 - \delta)/2]$  for  $T=0.1J$ . These are exactly the positions of the IAF peaks determined by the dispersion of very well defined renormalized spin excitations. Since the height of the IAF peaks is determined by damping, it is fully understandable that they are suppressed as the neutron energy  $\omega$  and temperature are increased. The novel result of this paper, namely, the shift of the position for IAF peaks as the temperature increases is also due to the same reason. To demon-

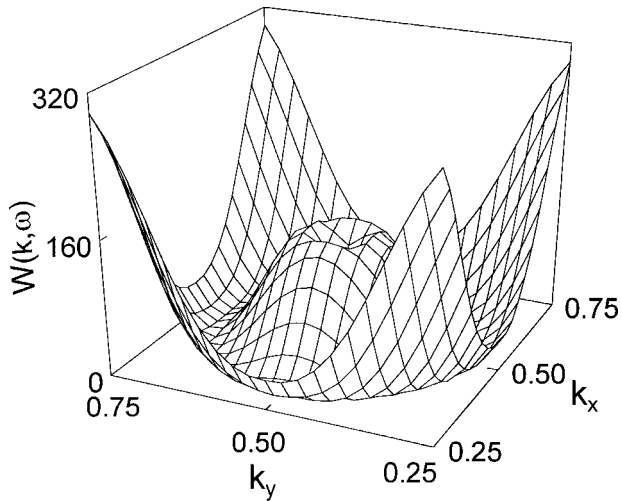


FIG. 5. Function  $W(\mathbf{k}, \omega)$  in the  $(k_x, k_y)$  plane at doping  $x = 0.06$  for parameter  $t/J = 2.5$  and energy  $\omega = 0.1J$  at temperature  $T = 0.1J$ .

strate this point in Fig. 6, we plot the function  $W(\mathbf{k}, \omega)$  along the arc from  $\mathbf{k} = [(1-\delta)/2, 1/2]$  via  $[(1-\delta/\sqrt{2})/2, (1-\delta/\sqrt{2})/2]$  to  $[1/2, (1-\delta)/2]$  at doping  $x = 0.06$  for  $t/J = 2.5$  and  $\omega = 0.05J$  for different temperatures  $T = 0.1J$  (solid line),  $T = 0.2J$  (dashed line),  $T = 0.4J$  (dash-dotted line), and  $T = 0.5J$  (dotted line) which shows clearly the temperature dependence of the minima of  $W(\mathbf{k}, \omega) - \mathbf{k}_\delta$ . This means the self-energy correction due to holon motion is temperature dependent. From the physical point of view, this is very reasonable. It would be of great interest to check explicitly this prediction in neutron experiments at much higher temperatures.

To conclude we have shown very clearly in the paper that if the local single occupancy constraint is treated properly (as done in the fermion-spin theory) and the strong spinon-holon interaction is taken into account, the  $t$ - $J$  model per se can correctly reproduce all main features of IAF in underdoped cuprates, including the doping dependence of the IAF peak position and the energy as well as temperature dependence of the amplitude of these peaks, without using adjustable pa-

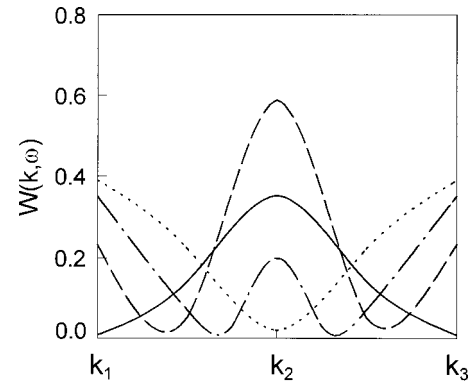


FIG. 6. Function  $W(\mathbf{k}, \omega)$  from  $\mathbf{k}_1 = [(1-\delta)/2, 1/2]$  via  $\mathbf{k}_2 = [(1-\delta/\sqrt{2})/2, (1-\delta/\sqrt{2})/2]$  to  $\mathbf{k}_3 = [1/2, (1-\delta)/2]$  at doping  $x = 0.06$  for parameter  $t/J = 2.5$  and energy  $\omega = 0.05J$  at temperatures  $T = 0.1J$  (solid line),  $T = 0.2J$  (dashed line),  $T = 0.4J$  (dash-dotted line), and  $T = 0.5J$  (dotted line).

rameters. We believe these are universal features of the underdoped cuprates, as shown by experiments on  $\text{La}_{2-x}\text{Sr}_x\text{CuO}_4$ ,<sup>4,12</sup>  $\text{La}_2\text{CuO}_{4+x}$ ,<sup>20</sup> and  $\text{YBa}_2\text{Cu}_3\text{O}_{7-x}$ .<sup>5</sup> There might be additional features due to bilayer splitting in the band structure,<sup>21,5</sup> and related theoretical results will be presented elsewhere.<sup>22</sup> The theory also predicts a rotation of IAF peak position at very high temperatures which should be verified by future experiments.

Finally, we would like to mention that the influence of the additional second-neighbor hopping  $t'$  on the IAF and momentum-integrated dynamical spin susceptibility of the  $t$ - $J$  model has been discussed within the fermion-spin theory. It has been shown<sup>23</sup> that for small values of  $t'$  the qualitative behavior of the IAF and integrated dynamical susceptibility of the  $t$ - $t'$ - $J$  model is the same as obtained from the present  $t$ - $J$  model.

The authors would like to thank Professor T. Xiang for helpful discussions. This work was supported by the National Natural Science Foundation under Grant No. 10074007, and a Grant from the Ministry of Education of China.

<sup>1</sup>For reviews, see M.A. Kastner, R.J. Birgeneau, G. Shiran, and Y. Endoh, *Rev. Mod. Phys.* **70**, 897 (1998); A.P. Kampf, *Phys. Rep.* **249**, 219 (1994); T.E. Mason, cond-mat/9812287 (unpublished).  
<sup>2</sup>R.J. Birgeneau, Y. Endoh, Y. Hidaka, K. Kakurai, M.A. Kastner, T. Murakami, G. Shirane, T.R. Thurston, and K. Yamada, *Phys. Rev. B* **39**, 2868 (1989).  
<sup>3</sup>S.W. Cheong, G. Aeppli, T.E. Mason, H. Mook, S.M. Hayden, P.C. Canfield, Z. Fisk, K.N. Clausen, and J.L. Martinez, *Phys. Rev. Lett.* **67**, 1791 (1991).  
<sup>4</sup>K. Yamada, C.H. Lee, K. Kurahashi, J. Wada, S. Wakimoto, S. Ueki, H. Kimura, Y. Endoh, S. Hosoya, and G. Shirane, *Phys. Rev. B* **57**, 6165 (1998), and references therein.  
<sup>5</sup>P. Dai, H.A. Mook, R.D. Hunt, and F. Doğan, *Phys. Rev. B* **63**, 054525 (2001).

<sup>6</sup>A. Aharony, R.J. Birgeneau, A. Coniglio, M.A. Kastner, and H.E. Stanley, *Phys. Rev. Lett.* **60**, 1330 (1988); R.J. Gooding, N.M. Salem, R.J. Birgeneau, and F.C. Chou, *Phys. Rev. B* **55**, 6360 (1997).  
<sup>7</sup>J. Zaanen and O. Gunnarsson, *Phys. Rev. B* **40**, 7391 (1989); D. Poilblanc and T.M. Rice, *ibid.* **39**, 9749 (1989); H.J. Schulz, *Phys. Rev. Lett.* **64**, 1445 (1990).  
<sup>8</sup>C.L. Kane, P.A. Lee, T.K. Ng, B. Chakraborty, and N. Read, *Phys. Rev. B* **41**, 2653 (1990); B. Normand and P.A. Lee, *ibid.* **51**, 15 519 (1995).  
<sup>9</sup>N. Bulut, D. Hone, D.J. Scalapino, and N.E. Bickers, *Phys. Rev. Lett.* **64**, 2723 (1990); Q. Si, Y. Zha, K. Levin, and J.P. Lu, *Phys. Rev. B* **47**, 9055 (1993); T. Tanamoto, H. Kohno, and H. Fukuyama, *J. Phys. Soc. Jpn.* **63**, 2739 (1994); Y. Hasegawa and H.

- Fukuyama, Jpn. J. Appl. Phys. **26**, L322 (1987).
- <sup>10</sup>C.M. Varma, P.B. Littlewood, S. Schmitt-Rink, E. Abrahams, and A.E. Ruckenstein, Phys. Rev. Lett. **63**, 1996 (1989).
- <sup>11</sup>P.B. Littlewood, J. Zaanen, G. Aeppli, and H. Monien, Phys. Rev. B **48**, 487 (1993).
- <sup>12</sup>G. Aeppli, T.E. Mason, S.M. Hayden, H.A. Mook, and J. Kulda, Science **278**, 1432 (1997).
- <sup>13</sup>S. Sachdev and J. Ye, Phys. Rev. Lett. **69**, 2411 (1992); S. Sachdev, C. Buragohain, and M. Vojta, Science **286**, 2479 (1999).
- <sup>14</sup>E. Dagotto, Rev. Mod. Phys. **66**, 763 (1994), and references therein.
- <sup>15</sup>Shiping Feng, Z.B. Su, and L. Yu, Phys. Rev. B **49**, 2368 (1994); Mod. Phys. Lett. B **7**, 1013 (1993).
- <sup>16</sup>D. Arovas and A. Auerbach, Phys. Rev. B **38**, 316 (1988); D. Yoshioka, J. Phys. Soc. Jpn. **58**, 32 (1989); see also, L. Yu, in *Recent Progress in Many-Body Theories*, edited by T.L. Ainsworth, C.E. Campbell, B.E. Clements, and E. Krotscheck (Plenum, New York, 1992), Vol. 3, p. 157.
- <sup>17</sup>Shiping Feng and Zhongbing Huang, Phys. Rev. B **57**, 10 328 (1998).
- <sup>18</sup>Shiping Feng and Yun Song, Phys. Rev. B **55**, 642 (1997).
- <sup>19</sup>J. Kondo and K. Yamaji, Prog. Theor. Phys. **47**, 807 (1972).
- <sup>20</sup>B.O. Wells, Y.S. Lee, M.A. Kastner, R.J. Christianson, R.J. Birgeneau, K. Yamada, Y. Endoh, and G. Shirane, Science **277**, 1067 (1997); Y.S. Lee, R.J. Birgeneau, M.A. Kastner, Y. Endoh, S. Wakimoto, K. Yamada, R.W. Erwin, and S.H. Lee, Phys. Rev. B **60**, 3643 (1999).
- <sup>21</sup>D.L. Feng, N.P. Armitage, D.H. Lu, A. Damascelli, J.P. Hu, P. Bogdanov, A. Lanzara, F. Ronning, K.M. Shen, H. Eisaki, C. Kim, Z.-X. Shen, J.-i. Shimoyama, and K. Kishio, Phys. Rev. Lett. **86**, 5550 (2001).
- <sup>22</sup>Shiping Feng, Feng Yuan, Zhao-Bin Su, and Lu Yu (unpublished).
- <sup>23</sup>Ying Liang and Shiping Feng (unpublished); Xianglin Ke, Feng Yuan, and Shiping Feng, Phys. Rev. B **62**, 134 (2000).